ChemComm

COMMUNICATION

View Article Online
View Journal | View Issue

Cite this: *Chem. Commun.*, 2018, **54**, 8371

Received 14th June 2018,
Accepted 2nd July 2018

DOI: 10.1039/c8cc04708a

rsc.li/chemcomm

ProTide generated long-acting abacavir nanoformulations†

Zhiyi Lin,[ab] Nagsen Gautam,[b] Yazen Alnouti,[b] JoEllyn McMillan,[a] Aditya N. Bade,[a] Howard E. Gendelman *[ab] and Benson Edagwa*[a]

Abacavir pronucleotide nanoformulations (NM3ABC) were prepared as a novel long acting slow effective release antiretroviral therapy. Single NM3ABC treatment of human monocyte-derived macrophages produced sustained intracellular carbovir-triphosphate and antiretroviral activities for up to 30 days.

The translation of long acting slow effective release antiretroviral therapy (LASER ART) from laboratory research into clinical practice could improve human immunodeficiency virus (HIV) prevention and treatment and inevitably speed up viral eradication efforts. The advantages of LASER ART over other antiretroviral regimens are defined by high antiretroviral drug (ARV) penetrance into cell and tissue viral reservoirs and infrequent dosing requirements. Both affect treatment outcomes by maximally suppressing viral growth through facilitated ARV entry into viral target cells.[1,2] Regimen adherence can be improved by reducing the dosing frequency. Indeed, recent data from our laboratories demonstrate that conversion of existing ARVs into prodrugs extends their apparent half-lives and reduces systemic drug toxicities.[3–6] However, while prodrugs represent >10% of all small molecules approved for human use, few have entered into HIV treatment regimens and none have appeared as part of long-acting ARV therapies.[7] Nonetheless, their advantages in facilitating drug biodistribution and extending drug half-lives is already known.[8]

Herein, ABC prodrugs were successfully developed by PRODrug and nucleoTIDE (ProTide) technology. While the idea was first introduced more than two and a half decades ago, the application of ProTide technology to abacavir (ABC) has focused on improving drug potency[9,10] not on extending its apparent half-life or on affecting viral reservoir biodistribution. To these ends, we implemented strategies to mask parent drug monophosphates with cleavable hydrophobic lipids creating ProTides that demonstrated improved plasma drug stability, membrane penetration and encapsulation. The synthesis and antiretroviral profiles of three ABC ProTides are described. One, **M3ABC**, was defined by efficient encasement into nanoparticles, production of high intracellular carbovir-triphosphate (CBV-TP) metabolites and superior monocyte-macrophage depot formation that enhanced antiretroviral activities.

Prior studies demonstrated that L-alanine and L-phenylalanine ester phosphoramidates provide potent ProTides.[10,11] Thus, we created **M1ABC** and **M2ABC** bearing alanine and phenylalanine methyl ester residues (Scheme 1 and Fig. 1A). **M3ABC** was synthesized by substituting the methyl ester in **M2ABC** for a docosyl ester promoiety. A docosanol masking ester motif was selected based

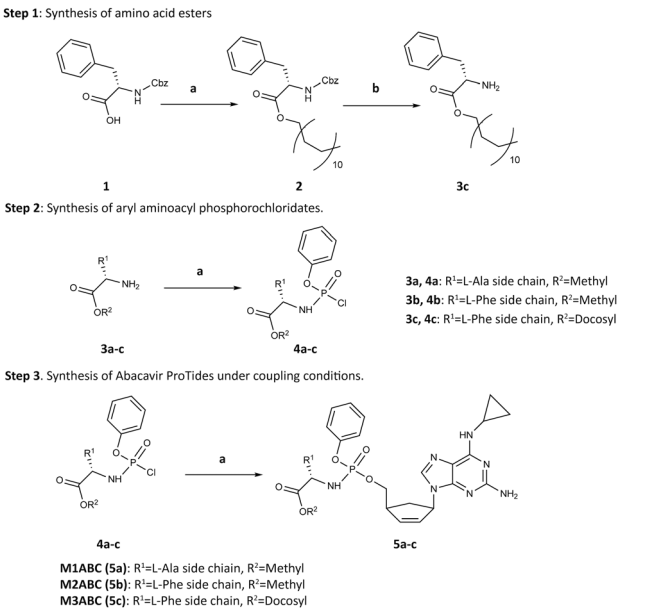

Scheme 1 Synthesis of ABC ProTides. *Reagent and conditions*: Step 1(a) 1-docosanol, HATU, imidazole, Et_3N, DMF/$CHCl_3$, 45 °C, 48 h; Step 1(b) Pd/C, Et_3SiH, MeOH/$CHCl_3$ (1 : 1 v/v), rt, 16 h. Step 2(a) phenyl dichlorophosphate, Et_3N, CH_2Cl_2, −78 °C–rt, 16 h. Step 3(a) ABC, *tert*-BuMgCl, THF, −78 °C–rt, 48–90 h.

[a] *Department of Pharmacology and Experimental Neuroscience, University of Nebraska Medical Center, Omaha, NE 68198-5880, USA. E-mail: hegendel@unmc.edu, benson.edagwa@unmc.edu*
[b] *Department of Pharmaceutical Science, University of Nebraska Medical Center, Omaha, NE 68198-5880, USA*

† Electronic supplementary information (ESI) available. See DOI: 10.1039/c8cc04708a

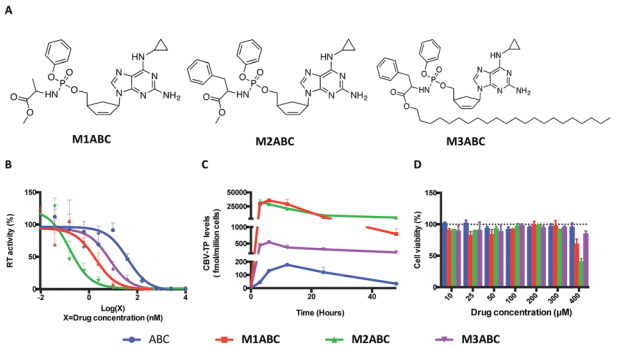

Fig. 1 The structure and biological characterization of ABC and its ProTides. (A) **M1ABC**, **M2ABC** and **M3ABC** were synthesized based on ProTide technology. (B) EC_{50} of ABC, **M1ABC**, **M2ABC** and **M3ABC** against HIV-1_{ADA} were determined in MDMs. (C) Intracellular CBV-TP levels were measured after MDMs were treated with 10 μM free ABC, **M1ABC**, **M2ABC** or **M3ABC** for various times. (D) Cytotoxicity of ABC, **M1ABC**, **M2ABC** and **M3ABC** in MDMs. Results are shown as percentage of cell viability as compared to untreated MDMs. Data are presented as mean ± SD for n = 3 samples per group.

on its lipophilicity, antiviral activities and inherent synergistic effect on nucleoside analogs.[12,13] ProTide hydrolysis was reasoned to release two pharmacophores that inhibit viral reverse transcriptase activity.[14] We reasoned that improving ABC physicochemical features would facilitate nanoformulation preparation, enhance intracellular ABC levels and extend the drugs' apparent half-life. The first step in the synthesis of ABC ProTides required preparation of aryl amino ester phosphorochloridates from appropriate amino acid esters and commercially available phenyl phosphorodichloridate.[15] Phenylalanine and alanine methyl esters were purchased while phenylalanine docosyl ester was prepared according to step 1 of Scheme 1. The aryl amino ester phosphorochloridates were then synthesized by coupling phenyl phosphorodichloridates to amino acid esters in the presence of triethylamine (Scheme 1 Step 2).[10] Each of the amino ester phosphorochloridates was then reacted with ABC in the presence of *tert*-butylmagnesium chloride and purified by flash column chromatography. This generated high yields of **M1ABC**, **M2ABC** and **M3ABC** (Scheme 1 Step 3, Fig. 1A). Successful synthesis of ABC ProTides was confirmed by ^{1}H, ^{13}C and ^{31}P NMR spectra (Fig. S1–S3, ESI†). As previously reported for similar compounds, splitting of the peaks in the spectra of ProTides was associated with the co-existence of two stereoisomers at the phosphorus atom.[16]

We next evaluated the ProTides for antiretroviral activity. As shown in Fig. 1B, **M1ABC**, **M2ABC** and **M3ABC** exhibited a 6- to 200-fold increase in antiretroviral activity over ABC in human monocyte-derived macrophages (MDMs). **M2ABC** demonstrated the lowest EC_{50} of 0.2 nM. The EC_{50} of **M1ABC** and **M3ABC** were 1.8 nM and 7.0 nM, respectively. The differences were likely linked to rapid prodrug uptake and metabolism of **M2ABC** to form CBV-TP[17,18] in MDM. Activation of ABC ProTides requires intracellular processing to generate CBV-TP.[10] To better explain the differences in EC_{50} between native ProTides and ABC, MDMs were exposed to equivalent concentrations of ABC, **M1ABC**, **M2ABC** or **M3ABC** followed by quantitation of CBV-TP levels at multiple time points.[9] As shown in Fig. 1C, the maximum CBV-TP levels for ABC, **M1ABC**, **M2ABC** and **M3ABC** were 177, 35650, 33135 and 541 fmol per million cells, respectively. At 48 h, the CBV-TP levels were 33, 789, 5025 and 230 fmol per million cells for ABC, **M1ABC**, **M2ABC** and **M3ABC**. The differences in active metabolite levels further suggest that the three ProTides are rapidly taken up by MDMs but metabolized at rates dependent on amino acid ester hydrolysis. Notably, at 48 h, the CBV-TP levels for **M3ABC** declined only by 57% compared to 81, 97 and 84% in the amount of active metabolite for ABC, **M1ABC** and **M2ABC** (Fig. S5, ESI†). We posit that enhanced lipophilicity and slower hydrolysis of **M3ABC** provides controlled and extended release of CBV-TP.

As intracellular nucleoside triphosphate levels have been implicated in drug toxicities,[19] we assessed the mitochondrial dehydrogenase activity of the ProTides using a CCK-8 assay. As shown in Fig. 1D, neither ABC, **M1ABC**, **M2ABC** nor **M3ABC** affected cell viability at drug concentrations of up to 300 μM. However, differences in mitochondrial activity were seen at 400 μM with **M1ABC** and **M2ABC** compared to ABC. No significant differences were observed between **M3ABC** and ABC across all tested drug concentrations. These data indicated that the sustained release of an effective inhibitory concentration of CBV-TP from **M3ABC** was not detrimental to cell viability and suggested that **M3ABC** could be translated for human use. Previous studies have shown that *in vivo* accumulation of nucleoside triphosphates inside cells could be facilitated by prodrugs that exhibit greater stability in plasma.[20,21] To evaluate prodrug stability, we incubated three ProTides in human serum. After 24 h, >60% of **M1ABC** and **M2ABC** was hydrolyzed. Nineteen percent of **M3ABC**, in contrast, was degraded after 24 h.

LASER ART was developed, in our laboratories, to improve therapeutic and prophylactic outcomes for HIV/AIDS. In the first phase this was accomplished by formulating myristoylated prodrugs encased in a poloxamer surfactant.[3–6] For ABC, such modifications provided only low levels of CBV-TP for less than two weeks.[5,22] We reasoned that ABC ProTide nanoformulations would produce higher levels of intracellular CBV-TP at substantially reduced dosing frequency. The less hydrophobic **M1ABC** was encapsulated into lipid-coated poly lactic-*co*-glycolic acid (PLGA) nanoparticles (N**M1ABC**) by a modified single emulsion solvent evaporation method while hydrophobic and lipophilic **M2ABC** and **M3ABC** ProTides were stabilized into poloxamer coated drug nanoparticles (N**M2ABC** and N**M3ABC**) by high-pressure homogenization.[23–25] The directive of both schemes was to produce controlled release drug delivery systems. The drug loadings for the N**M1ABC**, N**M2ABC** and N**M3ABC** nanoparticles were 3, 43, and 47%, respectively, underlying the differences between PLGA and poloxamer drug encasement systems. Indeed, unlike high-pressure homogenization that produces nanoparticles stabilized by surfactants with high drug loading, PLGA nanoparticles exhibit low drug loading.[23,26] Effective diameter (D_{eff}), polydispersity index (PdI), and ζ-potential were determined by dynamic light scattering (DLS) (Table S1, ESI†) while transmission electron microscopy (TEM) assessed nanoparticle morphologies (Fig. S6, ESI†). The nanoparticle morphologies for N**M1ABC** and N**M3ABC** were spherical with particle sizes of 135 nm and 230 nm, respectively, while N**M2ABC** particles were rod-shaped with a size of 265 nm. Importantly, high drug loading in N**M2ABC** and N**M3ABC** nanoformulations

can translate into reduced dosage volumes and minimal injection site reactions.[25]

Macrophage-drug interactions are demonstrated by LASER ART technologies. These have been shown to improve ART pharmacokinetics and pharmacodynamics by facilitating cell and tissue drug depots in the reticuloendothelial system.[27–29] Macrophages are outstanding targets for LASER ART due to their large storage capacity, their high mobility that allows entry to sites of infection and inflammation, and their role as viral reservoirs.[30,31] To affirm such observations, N**M1ABC**, N**M2ABC** and N**M3ABC** were administered to MDMs at concentrations of 100 μM. The intracellular prodrug concentrations were subsequently evaluated over 8 h. As shown in Fig. 2A, the highest drug nanoparticle MDM uptake was observed with N**M3ABC**. At 8 h, the intracellular prodrug concentration for N**M3ABC** was 118.5 nmol per 10^6 cells, a 56- and 108-fold higher concentration than that observed for N**M1ABC** (2.1 nmol per 10^6 cells) or N**M2ABC** (1.1 nmol per 10^6 cells), respectively. Visualization of nanoparticles within MDMs by TEM revealed greater accumulation of N**M3ABC** nanoparticles in the cytoplasmic vesicles compared to N**M1ABC** and N**M2ABC** (Fig. 2E). These observations likely reflect nanoparticle stability.[32] To further confirm the release of ProTides from the nanoparticles and their conversion to active metabolites, we quantified the intracellular CBV-TP levels in the MDMs after a single exposure to ABC, N**M1ABC**, N**M2ABC** or N**M3ABC**. As shown in Fig. 2B, the CBV-TP levels for ABC increased over time and peaked at 4 h (811 fmol per 10^6 cells) before declining by 37% (510 fmol per 10^6 cells) at 8 h. For N**M1ABC**, the maximum CBV-TP levels were observed at 8 h (39 533 fmol per 10^6 cells) while N**M2ABC** displayed the highest CBV-TP concentration of 39 015 fmol per 10^6 cells at 4 h followed by a 43% decrease (22 274 fmol per 10^6 cells) at 8 h. Even though lower concentrations of CBV-TP were measured for N**M3ABC** compared to N**M1ABC** or N**M2ABC**, the active metabolite levels were sustained over 8 h, ranging from 4626 to 8601 fmol per 10^6 cells *versus* 215 and 811 fmol per 10^6 cells for ABC. Conversion of **M3ABC** to CBV-TP demonstrates sustained drug release and could lead to improved patient adherence to therapeutic ARVs. To explore the potential of ProTide formulations to extend the apparent half-life of ABC, MDMs were exposed to formulations for 8 h. The intracellular ProTide and CBV-TP levels were measured over a 30-day time period. As shown in Fig. 2C, the amount of ProTide retained by MDM was undetectable for N**M1ABC** and N**M2ABC**, while N**M3ABC** exhibited drug concentrations of 95.3 and 48.5 nmol per 10^6 cells at days 1 and 30, respectively. The retention of CBV-TP in MDMs (Fig. 2D) was sustained until day 30 for N**M1ABC**, N**M2ABC** and N**M3ABC** but only detected to day 5 for ABC. Notably, a single treatment of MDMs with N**M3ABC** provided steady and sustained CBV-TP levels greater than 100 fmol per 10^6 cells over the entire

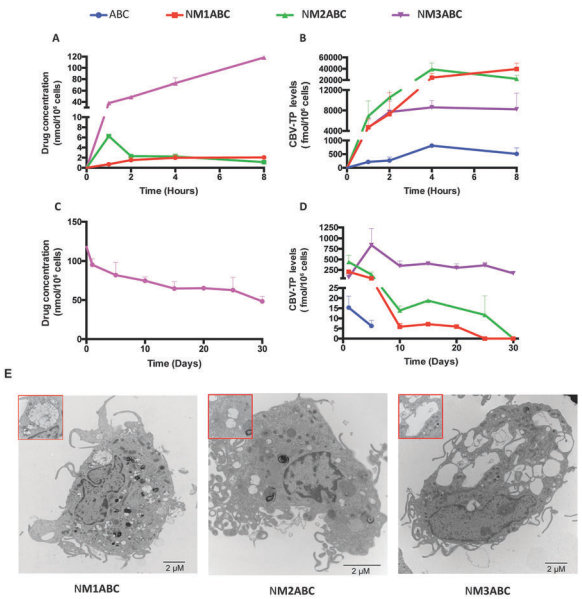

Fig. 2 Uptake and retention of the nanoformulations in MDMs. (A) and (B) For cell uptake, MDMs were treated with 100 μM ABC or prodrug nanoformulations for 1–8 h. (B) and (D) Drug retention in MDMs was determined after an 8 h drug loading followed by half media exchanges every other day for up to 30 days. Intracellular drug concentrations and CBV-TP levels were determined. Data are expressed as mean ± SD for n = 3 samples per group. (E) Transmission electron microscopy (TEM) was performed to visualize the morphologies of the formulation-loaded MDMs after 8 h incubation with nanoformulations.

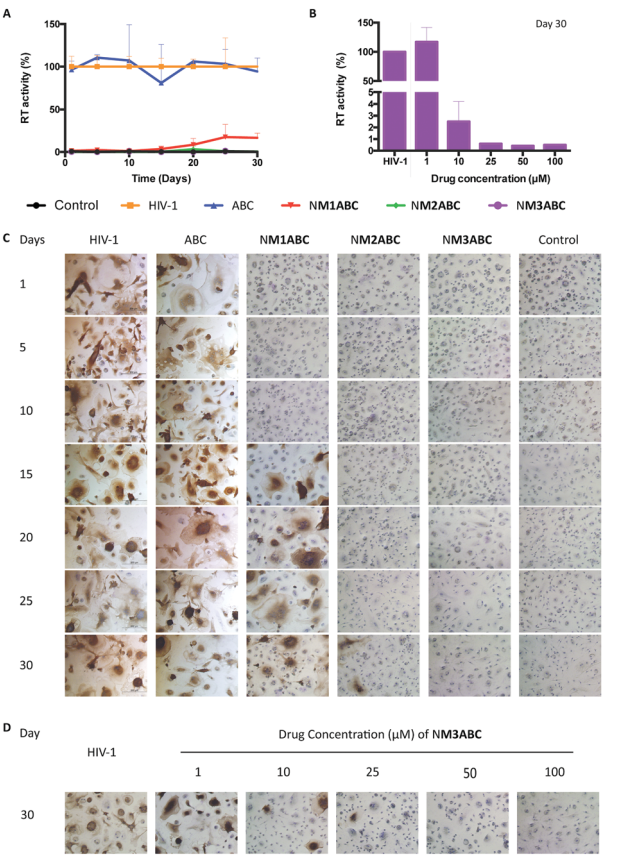

Fig. 3 ABC ProTide nanoformulations protect MDMs from HIV-1 infection over time. MDMs were treated with nanoformulations containing 100 μM ABC equivalent for 8 h. At predetermined time points, the MDMs were challenged with HIV-1_{ADA}. Samples were collected for antiretroviral activity assessment ten days after viral challenge by (A) measuring HIV RT activities and (C) staining HIV-1p24 antigen. (B) and (D) MDMs were treated with 1, 10, 25, 50 and 100 μM N**M3ABC** for 8 h. At day 30 post treatment, the MDMs were challenged with HIV-1_{ADA}. Ten days after infection, the culture media were collected for RT assay and the cells were fixed and stained for HIV-1p24 antigen. Data are expressed as mean ± SD for n = 3 samples per group.

30 day period. Such sustained release formulations could minimize variant pharmacokinetic profiles and maintain effective drug concentrations at cellular and tissue reservoirs of infection.

To determine whether sustained intracellular CBV-TP from ProTide formulations would translate into improved antiretroviral activity, MDMs were challenged with HIV-1_{ADA} for up to 30 days after a single 8 h treatment with 100 μM of ABC equivalent. HIV-1 reverse transcriptase (RT) activity and p24 antigen expression were assessed in infectious supernatants and adherent MDMs on day 10 post-infection. As shown in Fig. 3A and C, complete viral inhibition was observed for up to 15 days for N**M1ABC**. At day 20, 91% viral inhibition was recorded that gradually decreased to 83% inhibition at day 30. HIV-1p24 antigen staining showed that N**M2ABC** protected MDM from infection with viral breakthrough at day 30. Of significance, full viral inhibition was observed for 30 days after treatment with N**M3ABC**. In contrast, minimal protection against viral infection was observed with native ABC at all time points. Comparisons of antiviral efficacy of N**M3ABC** were then assessed to determine the lowest drug concentration required for long-term MDM protection against viral infection. As shown in Fig. 3B and D, 50 μM N**M3ABC** afforded complete viral inhibition for up to 30 days, while a single 8 h treatment with 25 μM or 10 μM N**M3ABC** inhibited viral replication by greater than 90% at day 30 post drug treatment. These results paralleled prolonged high intracellular CBV-TP levels for N**M3ABC** compared to ABC, N**M1ABC** or N**M2ABC**.

A pilot *in vivo* study in rats was conducted with N**M3ABC**. Peripheral blood mononuclear cells were recovered from whole blood and the intracellular CBV-TP levels measured at day 7 (Table S2, ESI†). Reduced CBV-TP levels are explained, in part, by the rapid degradation of ProTides or slow cleavage of phosphoramide intermediates in rodents that precedes triphosphate formation.[33]

In conclusion, we posit that LASER ART can overcome challenges of ARV adherence and biodistribution. In support of this idea, **M1ABC**, **M2ABC** and **M3ABC** ProTides were synthesized. N**M3ABC** nanoparticles exhibited improved MDM drug uptake, sustained retention and antiretroviral activities for up to one month. We posit that this work is a significant step forward for the management and prevention of HIV-1 infection.

The research was supported by the University of Nebraska Foundation and the National Institutes of Health grants R01 MH104147, P01 DA028555, R01 NS36126, P01 NS31492, 2R01 NS034239, P01 MH64570, P30 MH062261, P30 AI078498, and R01 AG043540.

Conflicts of interest

There are no conflicts to declare.

Notes and references

1 B. Edagwa, J. McMillan, B. Sillman and H. E. Gendelman, *Expert Opin. Drug Delivery*, 2017, **14**, 1281–1291.
2 R. J. Landovitz, R. Kofron and M. McCauley, *Curr. Opin. HIV AIDS*, 2016, **11**, 122–128.
3 B. Sillman, A. N. Bade, P. K. Dash, B. Bhargavan, T. Kocher, S. Mathews, H. Su, G. D. Kanmogne, L. Y. Poluektova and S. Gorantla, *Nat. Commun.*, 2018, **9**, 443.
4 T. Zhou, H. Su, P. Dash, Z. Lin, B. L. D. Shetty, T. Kocher, A. Szlachetka, B. Lamberty, H. S. Fox and L. Poluektova, *Biomaterials*, 2018, **151**, 53–65.
5 D. Singh, J. McMillan, J. Hilaire, N. Gautam, D. Palandri, Y. Alnouti, H. E. Gendelman and B. Edagwa, *Nanomedicine*, 2016, **11**, 1913–1927.
6 D. Guo, T. Zhou, M. Araínga, D. Palandri, N. Gautam, T. Bronich, Y. Alnouti, J. McMillan, B. Edagwa and H. E. Gendelman, *JAIDS, J. Acquired Immune Defic. Syndr.*, 2017, **74**, e75–e83.
7 J. Rautio, N. A. Meanwell, L. Di and M. J. Hageman, *Nat. Rev. Drug Discovery*, 2018, DOI: 10.1038/nrd.2018.46 [Epub ahead of print].
8 K. M. Huttunen, H. Raunio and J. Rautio, *Pharmacol. Rev.*, 2011, **63**, 750–771.
9 J. Balzarini, S. Aquaro, A. Hassan-Abdallah, S. M. Daluge, C. F. Perno and C. McGuigan, *FEBS Lett.*, 2004, **573**, 38–44.
10 C. McGuigan, S. A. Harris, S. M. Daluge, K. S. Gudmundsson, E. W. McLean, T. C. Burnette, H. Marr, R. Hazen, L. D. Condreay, L. Johnson, E. De Clercq and J. Balzarini, *J. Med. Chem.*, 2005, **48**, 3504–3515.
11 C. McGuigan, K. G. Devine, T. J. O'Connor and D. Kinchington, *Antiviral Res.*, 1991, **15**, 255–263.
12 D. H. Katz, J. F. Marcelletti, L. E. Pope, M. H. Khalil, L. R. Katz and R. McFadden, *Ann. N. Y. Acad. Sci.*, 1994, **724**, 472–488.
13 J. F. Marcelletti, *Antiviral Res.*, 2002, **56**, 153–166.
14 C. Piantadosi, C. J. Marasco, Jr., S. L. Morris-Natschke, K. L. Meyer, F. Gumus, J. R. Surles, K. S. Ishaq, L. S. Kucera, N. Iyer and C. A. Wallen, *et al.*, *J. Med. Chem.*, 1991, **34**, 1408–1414.
15 D. Cahard, C. McGuigan and J. Balzarini, *Mini-Rev. Med. Chem.*, 2004, **4**, 371–381.
16 S. Kandil, J. Balzarini, S. Rat, A. Brancale, A. D. Westwell and C. McGuigan, *Bioorg. Med. Chem. Lett.*, 2016, **26**, 5618–5623.
17 R. D. Hanson, P. A. Hohn, N. C. Popescu and T. J. Ley, *Proc. Natl. Acad. Sci. U. S. A.*, 1990, **87**, 960–963.
18 G. Birkus, N. Kutty, G. X. He, A. Mulato, W. Lee, M. McDermott and T. Cihlar, *Mol. Pharmacol.*, 2008, **74**, 92–100.
19 T. N. Kakuda, *Clin. Ther.*, 2000, **22**, 685–708.
20 W. A. Lee, G. X. He, E. Eisenberg, T. Cihlar, S. Swaminathan, A. Mulato and K. C. Cundy, *Antimicrob. Agents Chemother.*, 2005, **49**, 1898–1906.
21 R. L. Mackman, A. S. Ray, H. C. Hui, L. Zhang, G. Birkus, C. G. Boojamra, M. C. Desai, J. L. Douglas, Y. Gao, D. Grant, G. Laflamme, K. Y. Lin, D. Y. Markevitch, R. Mishra, M. McDermott, R. Pakdaman, O. V. Petrakovsky, J. E. Vela and T. Cihlar, *Bioorg. Med. Chem.*, 2010, **18**, 3606–3617.
22 N. Gautam, Z. Lin, M. G. Banoub, N. A. Smith, A. Maayah, J. McMillan, H. E. Gendelman and Y. Alnouti, *J. Pharm. Biomed. Anal.*, 2018, **153**, 248–259.
23 T. Zhou, Z. Lin, P. Puligujja, D. Palandri, J. Hilaire, M. Arainga, N. Smith, N. Gautam, J. McMillan, Y. Alnouti, X. Liu, B. Edagwa and H. E. Gendelman, *Nanomedicine*, 2018, **13**, 871–885.
24 Y. Liu, K. Li, J. Pan, B. Liu and S. S. Feng, *Biomaterials*, 2010, **31**, 330–338.
25 Z. Lin and H. E. Gendelman, in *Encyclopedia of AIDS*, ed. T. J. Hope, M. Stevenson and D. Richman, Springer New York, New York, NY, 2016, pp. 1–10, DOI: 10.1007/978-1-4614-9610-6_220-1.
26 J. Xu, S. Zhang, A. Machado, S. Lecommandoux, O. Sandre, F. Gu and A. Colin, *Sci. Rep.*, 2017, **7**, 4794.
27 D. P. Gnanadhas, P. K. Dash, B. Sillman, A. N. Bade, Z. Lin, D. L. Palandri, N. Gautam, Y. Alnouti, H. A. Gelbard, J. McMillan, R. L. Mosley, B. Edagwa, H. E. Gendelman and S. Gorantla, *J. Clin. Invest.*, 2017, **127**, 857–873.
28 P. Puligujja, S. S. Balkundi, L. M. Kendrick, H. M. Baldridge, J. R. Hilaire, A. N. Bade, P. K. Dash, G. Zhang, L. Y. Poluektova, S. Gorantla, X. M. Liu, T. Ying, Y. Feng, Y. Wang, D. S. Dimitrov, J. M. McMillan and H. E. Gendelman, *Biomaterials*, 2015, **41**, 141–150.
29 B. J. Edagwa and H. E. Gendelman, *Nat. Mater.*, 2018, **17**, 114–116.
30 M. Arainga, B. Edagwa, R. L. Mosley, L. Y. Poluektova, S. Gorantla and H. E. Gendelman, *Retrovirology*, 2017, **14**, 17.
31 M. Arainga, D. Guo, J. Wiederin, P. Ciborowski, J. McMillan and H. E. Gendelman, *Retrovirology*, 2015, **12**, 5.
32 S. Kumar, A. C. Anselmo, A. Banerjee, M. Zakrewsky and S. Mitragotri, *J. Controlled Release*, 2015, **220**, 141–148.
33 M. Slusarczyk, M. H. Lopez, J. Balzarini, M. Mason, W. G. Jiang, S. Blagden, E. Thompson, E. Ghazaly and C. McGuigan, *J. Med. Chem.*, 2014, **57**, 1531–1542.

